

Shahrood University of  
Technology



Iranian Society of  
Mining Engineering  
(IRISME)

# Assessing Blasting-Induced Noise in Open Pit Mining: A Comparative Approach Using Analytical Models and Machine Learning

Zaenal Zaenal, Noor Fauzi Isnarno, Delina Mutiara, Delina Mutiara, Sofie Nur'aini, Hasyim Fadhilah, Elfida Moralista and Andrianto Nurrochman\*

Department of Mining Engineering, Faculty of Engineering, Universitas Islam Bandung, Bandung, Indonesia

## Article Info

Received 15 August 2025

Received in Revised form 30  
September 2025

Accepted 14 December 2025

Published online 15 December 2025

DOI: [10.22044/jme.2025.16675.3271](https://doi.org/10.22044/jme.2025.16675.3271)

## Keywords

Blasting noise

Machine learning

Environmental impact

Noise prediction models

## Abstract

Blasting is a fundamental open-pit mining operation necessary for rock breakage, but it also generates significant environmental noise pollution. Excessive noise from blasting not only endangers health but also poses problems to compliance with regulations, particularly in regions where acoustic standards differ, such as Indonesia's use of both dBL and dBA standards. This research addresses the need for reliable and context-dependent predictive models for blasting noise, aiming to compare analytical and empirical formulas with machine learning techniques in dBA prediction. Measurements were conducted at 30 blasts at an open-pit coal mine in Indonesia, South Sumatra, using homogeneous acoustic sensors. The measured data points for frequency, dBL, and dBA were matched to calculated data using equations. Random Forest (RF) and Artificial Neural Network (ANN) predictive models using measured frequency and dBL as predictive variables were also derived. Results show that used Finn-derived equation has poor predictive accuracy, with errors exceeding 80%. Among the analytical and empirical models, Equation 3 performed the best, with an average error of 9%, while a site-specific regression model based on measurements had an improved error rate of 5%. Machine learning models outperformed all models, with the RF model exhibiting an average error of 2% and demonstrating higher stability and consistency. The ANN model also did well, but with more variation and some overestimations.

## 1. Introduction

Blasting is one of the primary methods used in mining activities to break rock masses. However, besides producing the desired rock fragmentation, blasting activities also pose environmental impacts, one of which is noise pollution [1-4]. The noise levels generated by blasting activities are of significant concern, as they can impact the health of workers and the surrounding community, potentially causing substantial environmental disturbances.

Noise in the mining industry is one of the most prevalent environmental issues. Equipment such as drilling rigs, loaders, trucks, bulldozers, crushers, screens, and other frequently used equipment in surface mining, as well as blasting activities, is inherently noisy. Consequently, noise has long been recognized as a risk to employees at mining

operation sites and the surrounding environment [5,2,6,7]. Blasting noise, in particular, extends beyond being merely an environmental issue; it is transforming into a multifaceted socio-technical concern that directly impacts operational effectiveness, corporate social responsibility, and risk compliance. When open-pit mines are located near residential areas, the number of affected populations can be greater, and the hazard risk is not always limited to employees alone, with all its associated consequences.

The most common adverse health effects related to prolonged exposure to noise include sleep disorders, learning impairments, hypertension, and ischemic heart disease. For instance, Mocek et al. [6] highlighted how noise from mining activities significantly contributes to the increase in sleep



disorder cases among populations living near open-pit mines. Additionally, research by Persson et al. [8] found that low-frequency noise, which is dominant in mining activities, can indirectly affect the human nervous system, impacting productivity and mental health among mine workers.

Workers exposed to prolonged noise levels often experience fatigue, reduced concentration, and increased irritability, which ultimately affect their overall work productivity. Moreover, noise pollution can disrupt communication in mining environments [7,5,6], posing significant safety risks during critical operations. These health effects may lead to complaints and legal issues. Consequently, these problems can cause delays or shutdowns in operations and shift the concern from being solely environmental to becoming a direct financial and operational issue.

To address these impacts, the mining industry has relied on predictive models. These approaches have undergone significant evolution from conventional analytical formulas to modern data-driven methods. Traditionally, analytical models have served as the foundation for predicting noise generated by explosions. These models are typically based on the explosive charge per delay (W) and the distance to the monitoring location (R) [9-12]. However, despite incorporating key physical parameters, the predictive reliability of these models remains limited. Field studies by Lee et al. [2] have consistently shown that many site-specific variables introduce uncertainties and are difficult to account for in standard predictive models. Such variables include stemming length, rock properties, meteorological conditions, and topography.

Atmospheric conditions, including wind speed and direction, temperature, and barometric pressure, further complicate the dynamics of noise dispersion. As a result, even well-calibrated empirical models often fail to deliver consistent predictions under varying environmental and operational conditions. Because of these unreliabilities, direct practical consequences frequently require excessively conservative safety factors to comply with regulations. This practice, though reasonable, ultimately reduces blasting efficiency, lengthens project durations, and raises expenses. The necessity for regulations compliance is broadly seen as scientifically deficient. This reveals an ongoing gap among scientific knowledge, industry practices, and regulatory frameworks that becomes a fundamental issue that continues to hinder effective execution.

In response to these drawbacks, recent studies [13-19] have increasingly proposed applying machine learning (ML) prediction methods to identify noise propagation patterns more dynamically and adaptively. ML techniques have emerged as a superior approach for addressing the limitations of analytical models. They effectively capture the complex, non-linear relationships among numerous influencing factors [20]. Various algorithms, such as Artificial Neural Networks (ANN) [13], Random Forests (RF) [21], and Support Vector Machines (SVM) [22], have already demonstrated effectiveness in predicting various blast-induced impacts. More recently, researchers have explored advanced hybrid models. For example, combinations like XGBoost with Grey Wolf Optimization (GWO) and CatBoost paired with the Butterfly Optimization Algorithm (BOA) have shown impressive predictive accuracy, with coefficients of determination ( $R^2$ ) exceeding 0.98 in some cases [23].

Despite their superiority in data prediction, ML often face criticism due to the complexity of their structure, which can make it challenging to clarify precisely physical interpretability [24]. Nevertheless, the continuous discussion on whether to emphasize clear interpretability or enhance predictive accuracy is not insignificant. Regulatory must contend with these conflicting priorities, and addressing this conflict is far from simple [25]. An analytical and empirical model offers transparency in its formulation. However, its predictions are unreliable and suffer from predictive deficiencies that may provide incorrect justification. Consequently, for critical applications like maintaining compliance with environmental noise regulations, the main necessity for a predictive tool is its proven accuracy and reliability.

Despite notable progress, substantial gaps in research remain. In regions with a complex legal system, one persistent issue exists about the misalignment between field acoustic measurement practices and the requirements set by regulatory frameworks. In the Indonesian context, Standar Nasional Indonesia (SNI) 7570:2023 provides technical guidelines for measuring blast-induced noise, emphasizing the use of linear sound pressure levels, expressed in decibels linear (dBL). Conversely, regulatory frameworks issued by the Ministry of Environment and Forestry (Kementerian Lingkungan Hidup dan Kehutanan – KLHK) in Indonesia require noise evaluations to be reported in A-weighted decibels (dBA), which

are more representative of human auditory sensitivity across different frequencies.

To reconcile these differing standards, SNI 7570:2023 incorporates the A-weighting correction method proposed by Finn [26], enabling the conversion of dBL to dBA. Nevertheless, this methodological divergence introduces technical challenges in the acquisition, interpretation, and regulatory validation of acoustic data. The need to navigate between instrument-measured linear values and perceptually weighted metrics underscores the importance of harmonizing measurement protocols and enhancing analytical accuracy in environmental noise assessments within mining operations. The majority of current research contrasts one or two ML models with a single analytical or empirical formula. There is a significant lack of studies that conduct a thorough, simultaneous comparison among a wide range of models [13]. A thorough benchmark requires evaluating several established analytical and empirical models, site-adjusted models, and diverse ML frameworks, all assessed on a uniform, consistent dataset within a detailed and complex operational environment.

This study aims to address these critical gaps. It empirically evaluates a nationally standardized acoustic conversion methodology. The research provides a comprehensive, field-based comparative analysis of several analytical approaches, including the derived Finn equation, three established analytical and empirical formulas, a site-specific regression model, and two machine learning architectures (Random Forest and Artificial Neural Network). Each model is assessed

for its ability to predict dBA levels within the framework of Indonesian regulatory requirements. This represents the first time such a detailed, data-driven comparison has been conducted in this specific context.

By understanding the noise patterns caused by blasting, this research aims to offer more effective recommendations for controlling environmental impacts in mining blasting activities. Effective noise management in mining operations requires a comprehensive understanding of noise sources, accurate prediction models, and practical mitigation strategies. This study provides essential insights to enhance environmental sustainability and offers a scientific basis for stakeholders to support the reevaluation of national standards.

## 2. Methodology

### 2.1. Site Characterization and Environmental Conditions

#### 2.1.1. Study Area

The research location is situated in the operational area of PT Bukit Asam Tbk, a major open-pit coal mine in Tanjung Enim, Muara Enim Regency, South Sumatra Province, Indonesia, as shown in Figure 1. The research area encompasses active open-pit mining sites, including strategic points near heavy equipment areas, transportation routes, and nearby residential areas. Data collection points are selected representatively based on the varying levels of mining operational activity and the potential noise impact on the surrounding environment.

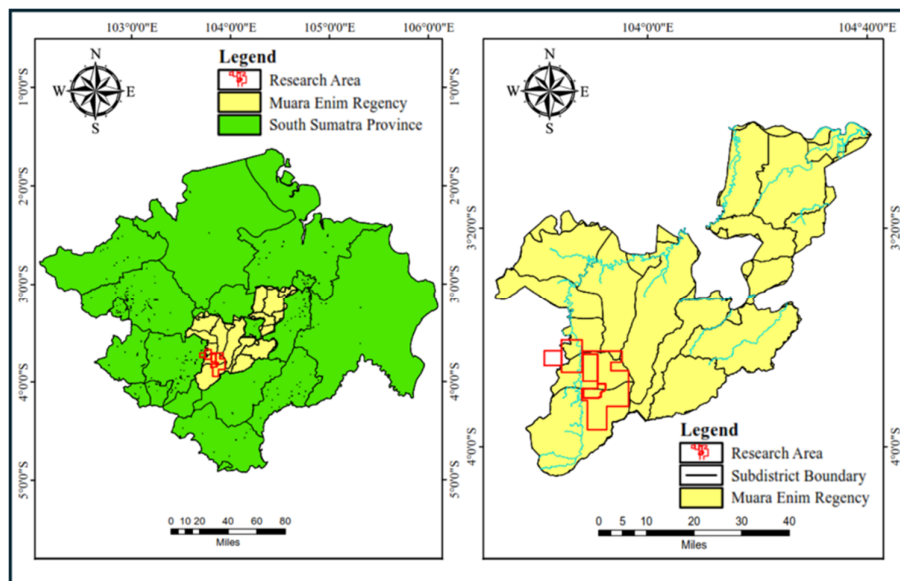


Figure 1. Research area location

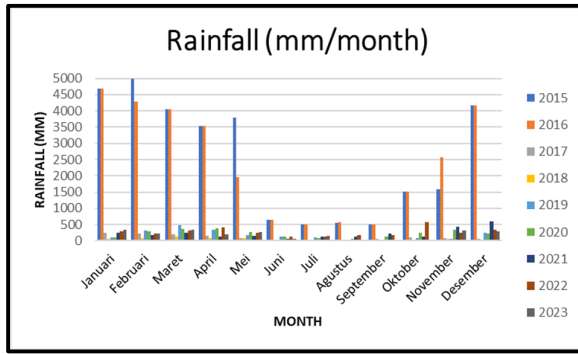


Figure 2. Rainfall distribution of the research area from 2015 to 2023

2.1.2. Geological and Geotechnical Framework

The geological conditions at the study area are a principal determinant of blast performance and are the principal series of uncontrollable variables in the study. The site location is within the South

Sumatra Basin, formed by tectonic activity between the subducting India-Australia plate and the Eurasian plate. During the extension phase, which lasted from the late Pre-Tertiary to the early Tertiary, the movement of the plates in the East-West direction was the most common in the basin. These basins are classified as foreland basins or back-arc basins geologically [27-31].

According to Darman and Sidi [32], subduction in the Sumatra region exhibits a unique pattern characterized by a clockwise rotation that accompanies changes in the orientation of the subduction zone. This pattern results in an oblique-oriented horizontal fault structure, which causes the complexity of the strain and stress system in the region, primarily due to the influence of the Sumatra Fault system. As shown in Figure 3, the Geological Map of the Lahat by Gafoer et al. [33] indicates that the research area is located around the Air Benakat Formation.

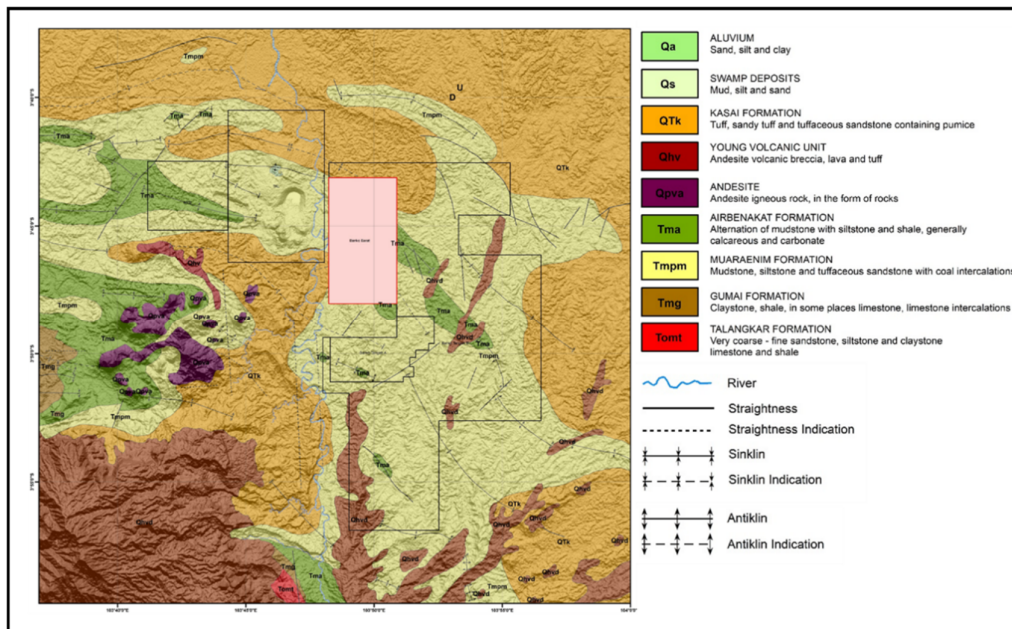


Figure 3. Geological Map of the Lahat Sheet by Gafoer et al. (1996)

According to Bishop [34], the South Sumatra basin geologically consists of Tertiary sedimentary rocks that unconformably overlie metamorphic basement rocks that were igneous in the Pre-Tertiary period. As can be seen in the Geological Map of the Lahat Sheet in Figure 3, the site of the study is in a series of sedimentary units, the Airbenakat Formation (Tma) and Muara Enim Formation (Tmpm) in majority. The local stratigraphy that is relevant to the blasting operation is:

Kasai Formation (QTk)

The Kasar Formation is a young layer located above the Muara Enim Formation of the Tertiary Quaternary age, consisting of coarse sandstone to conglomerate rock units. This formation was formed in a river or fluvial environment.

Airbenakat Formation (Tma)

This formation is of Miocene to Tertiary age, comprising sandstone, siltstone, and shale rock units. This formation reflects a transition from a

shallow marine to a delta transition sedimentary environment.

**Muara Enim Formation (Tmpm)**

This formation is of Late Miocene to Pliocene age, consisting of claystone, siltstone, and sandstone units with coal interbeds. The coal found in the Tmpm formation is known for its economically viable coal content.

Blasting activities in this study were done on hard and massive sedimentary rock mass similar to the nature of the Airbenakat and Kasai formations. These rock masses would typically exhibit sets of joints and bedding planes, significant discontinuities with a strong influence on the effectiveness of explosive energy transfer and formed fragmentation.

**2.1.3. Atmospheric Conditions**

Low-frequency acoustic energy propagation, such as noise generated from blasting, is sensitive to weather conditions. Conditions, including wind speed and direction, vertical temperature gradient, and relative humidity, can modulate measured sound pressure levels at a distance with the possibility of 10-20 dB variations [35]. Specifically, temperature inversion conditions, where increasing temperature with elevation, downwind propagation can cause downward refraction of sound waves. This converging acoustic energy amplifies sound at distant receptors. Conversely, temperature lapse conditions, which are typical of clear, sunny days, upwind propagation leads to upward refraction, which creates acoustic shadow zones and reduces sound levels [36].

To ensure that the noise measurements are reproducible and minimize the confounding impact of meteorological fluctuation, a basic assumption of the modeling of this study is that all measurements were taken under similar and comparable atmospheric conditions. In accordance with this assumption, all blasts were recorded at midday periods (10:00 to 14:00 local time) under good atmospheric conditions. Favorable conditions were considered as clear skies, absence of temperature inversion layers, and low mean wind speeds (below 5 m/s). This method constitutes the best operating practice for environmental noise measurement and was utilized to ensure that the observed fluctuations in measured noise could be attributed to parameters under control with minimal contribution from uncontrolled atmospheric factors.

**2.2. Blasting Design**

The design of blast geometry in mining blasting operations is crucial for the success and safety of the blasting process. To ensure optimal blast energy distribution, key parameters such as burden, spacing, drill hole depth, powder factor, and delay time must be considered. Moreover, the parameters for these blast sites under study were designed to minimize adverse off-site impacts. The geometric description of the blasting in this study is described in Figure 4 as follows:

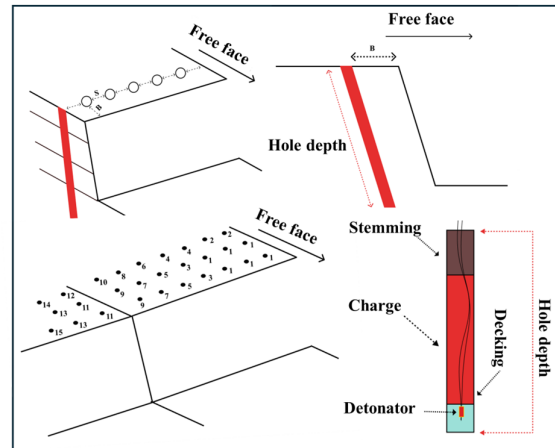


**Figure 4. Blasting geometric design**

**2.2.1. Blast Geometry Parameters**

In this study, the blast geometry design was set as presented in Table 1. Delay time is consistent with speeds of 42 m/s and 109 m/s. The adjustment of delay time is crucial for regulating the detonation sequence between holes, ensuring a successful fragmentation process without causing excessive pressure that could damage slope stability or trigger dangerous vibration spikes.

Design of blast geometry in this study was controlled by the operational imperative of prioritizing safety and minimizing environmental impacts at a minimum due to the proximity of the blasting sites to residential neighborhoods and other sensitive buildings [37]. Accordingly, the main objective was the implementation of a controlled blasting method to comply with stringent environmental regulations [38]. This approach acknowledges that over-confinement of explosives is a significant factor responsible for adverse effects such as high ground vibrations, airblast, and flyrock [39].

One of the major characteristics of this safety-oriented design is the use of a low total height to burden ratio (H/B) or burden stiffness ratio. For all 30 blasts, the H/B ratio was maintained at a

constant of 1.0. This is a short bench design that consciously deviates from ratios typically recommended for maximum fragmentation [40]. Low stiffness ratio is observed to cause less efficient energy use for fragmentation, with a tendency to produce larger fragments. This was, however, a design requirement to reduce the level of confinement on the explosive charge and the primary causes of airblast and ground vibration [39]. The resulting coarser but adequately fractured rock was deemed acceptable for subsequent mechanical excavation by shoveling, an efficient two-stage removal process for sensitive areas.

Similarly, the chosen Stemming-to-Burden (T/B) ratios of 0.47 to 0.78 were part of this safety-focused approach. They were believed to represent a balance between gas confinement and vibration restriction [41]. Over-stemming, on the other hand, improves confinement and can lead to higher ground vibrations [42]. The selected ratios of T/B were therefore site-specific compromises aimed at

developing sufficient confinement to fracture the rock mass without causing undesirable ground vibrations to the neighborhood community. Spacing-to-Burden (S/B) ratios were maintained within the optimal range of 1.17 to 1.20 to ensure good interaction among neighboring blastholes.

Blasting site locations are presented in Figure 5. Blasting was carried out on the overburden layer, the layer of cover rock that must be removed to access the primary source. The characteristics of overburden are usually hard and massive; therefore, the design of these blasting parameters is intended to achieve adequate fragmentation using efficient explosives while maintaining the stability of the work area and ensuring safety and environmental protection. This methodology reflects modern blasting practices in sensitive environments, where designs are frequently modified from production optimums to meet regulatory and social requirements [38].

**Table 1. Blasting geometry parameter**

| No | Blasting Geometry |            |             |              |                   | Total Depth (m) |
|----|-------------------|------------|-------------|--------------|-------------------|-----------------|
|    | Diameter (mm)     | Burden (m) | Spacing (m) | Stemming (m) | Column Charge (m) |                 |
| 1  | 158               | 5          | 6           | 3            | 2.09              | 5               |
| 2  | 158               | 5          | 6           | 3            | 2.09              | 5               |
| 3  | 158               | 6          | 7           | 3            | 2.09              | 6               |
| 4  | 158               | 6          | 7           | 3.6          | 1.77              | 6               |
| 5  | 158               | 6          | 7           | 3.6          | 1.77              | 6               |
| 6  | 158               | 6          | 7           | 3.6          | 1.77              | 6               |
| 7  | 158               | 6          | 7           | 3.6          | 1.77              | 6               |
| 8  | 158               | 6          | 7           | 3.6          | 1.77              | 6               |
| 9  | 158               | 6          | 7           | 3.6          | 1.77              | 6               |
| 10 | 158               | 6          | 7           | 3.6          | 1.77              | 6               |
| 11 | 158               | 6          | 7           | 3.6          | 1.77              | 6               |
| 12 | 158               | 6          | 7           | 3.6          | 1.77              | 6               |
| 13 | 158               | 6          | 7           | 3.6          | 1.77              | 6               |
| 14 | 158               | 6          | 7           | 3.6          | 1.77              | 6               |
| 15 | 158               | 6          | 7           | 3.6          | 1.77              | 6               |
| 16 | 158               | 6          | 7           | 3.6          | 1.77              | 6               |
| 17 | 158               | 6          | 7           | 3.6          | 1.77              | 6               |
| 18 | 158               | 6          | 7           | 3.6          | 1.77              | 6               |
| 19 | 158               | 6          | 7           | 3.6          | 1.77              | 6               |
| 20 | 158               | 6          | 7           | 3.6          | 1.77              | 6               |
| 21 | 158               | 6          | 7           | 3.6          | 1.77              | 6               |
| 22 | 158               | 6          | 7           | 3.6          | 1.77              | 6               |
| 23 | 158               | 6          | 7           | 3.6          | 1.77              | 6               |
| 24 | 158               | 6          | 7           | 3.6          | 1.77              | 6               |
| 25 | 158               | 6          | 7           | 3.6          | 1.77              | 6               |
| 26 | 158               | 6          | 7           | 3.6          | 1.77              | 6               |
| 27 | 158               | 6          | 7           | 2.8          | 2.09              | 6               |
| 28 | 158               | 6          | 7           | 2.8          | 2.09              | 6               |
| 29 | 158               | 6          | 7           | 3.9          | 2.09              | 6               |
| 30 | 158               | 6          | 7           | 3.9          | 2.09              | 6               |

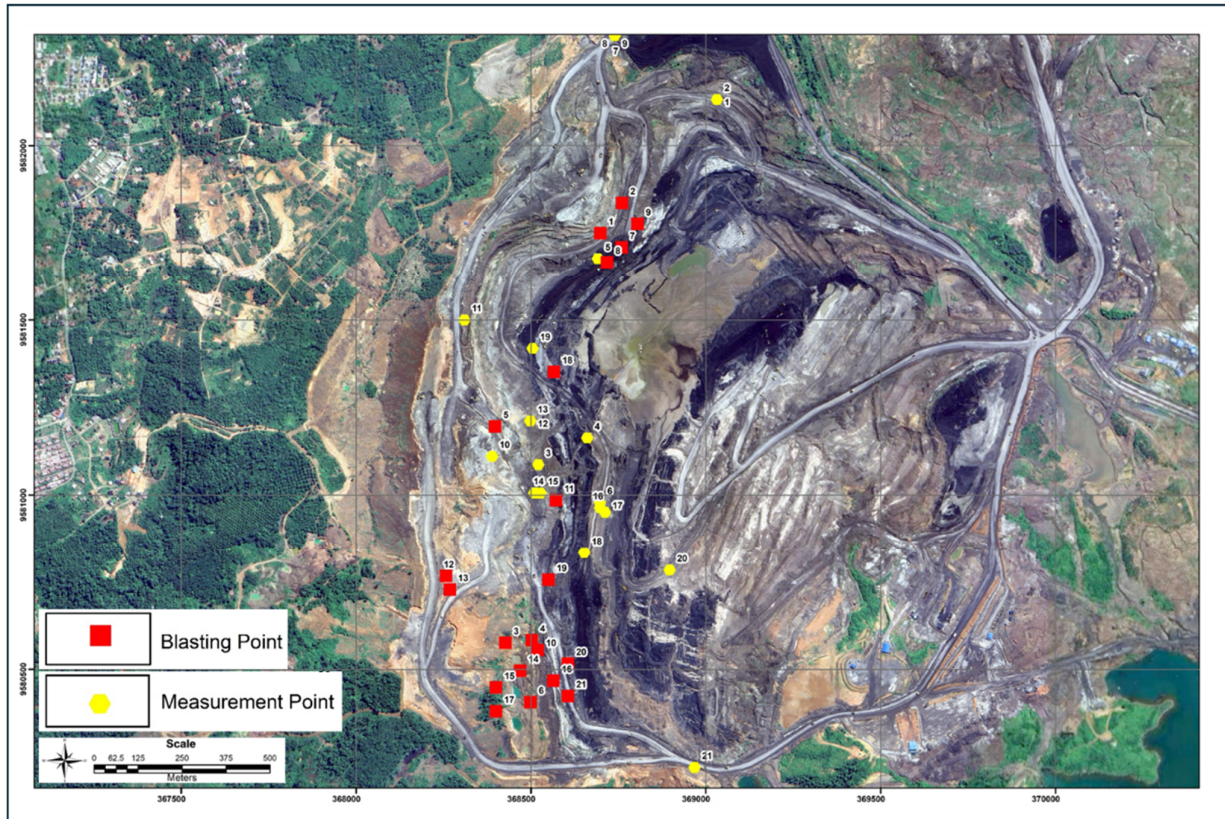


Figure 5. Blasting site location

**2.2.2. Explosive Properties and Powder Factor**

The entire blast holes were charged with Ammonium Nitrate Fuel Oil (ANFO), a widely used explosive in mining, which has a density of 0.85 g/cm<sup>3</sup>. ANFO was selected on the basis of its advantages, which are low cost, simplicity of production, and low sensitivity to mechanical shock on charging. The charge of the explosive was initiated from a non-electric initiation system made up of surface and in-hole delay detonators.

**2.3. Field Measurement**

**2.3.1. Instrumentation**

The measurement was conducted using an InstanTel Micromate seismograph, a specially designed instrument for recording blast-induced environmental effects. The seismograph was equipped with an ISEE-compliant linear microphone. The sensor has been specifically applied for measuring airblast. It possesses a flat frequency response from 2 Hz to 250 Hz, which is useful for effectively recording the low-frequency acoustic energy characteristic of air overpressure from large-scale blasting.

In the field, the microphone was placed on a tripod at a standard height of 1.2 m above the

ground to avoid near-ground interference effects. The microphone was directed at the blast location and fitted with a foam windscreen to minimize low-frequency noise caused by wind passing over the microphone diaphragm, which would otherwise contaminate the data. The monitoring unit was situated at a typical, secure distance of 500 m from the blasting site, in accordance with national safety standards, to capture far-field propagation effects. Coordinates for each measurement location were obtained with a hand-held GPS receiver. The data measurement plan and field layout are schematically illustrated in Figure 6 and Figure 7, respectively.

**2.3.2. Data Acquisition Parameters**

To ensure consistency and reproducibility, the acquisition parameters on the Micromate unit were standardized across all monitored events. The settings were chosen to align with international performance standards for seismograph blasting and best practices for monitoring air overpressure to produce high-fidelity data recordings. A trigger level of 110 dBL was selected as a conservative cut-off, significantly above normal ambient environment noise levels in the mining area but sufficiently sensitive to ensure no blast event was

missed. A sample rate of 2048 samples per second was used, more than twice the Nyquist frequency of the sensor's 250 Hz upper cutoff, to yield a high-resolution digital representation of the analogue pressure waveform. A fixed 5 s recording length

was used for all events, providing a sufficient time window to capture the entire transient air overpressure waveform, including the pre-event baseline for estimating ambient background noise and complete signal decay following the event.

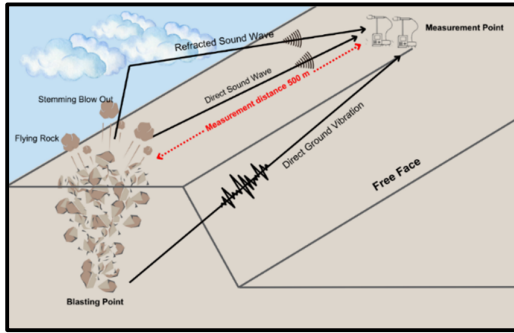


Figure 6. Blasting acoustic measurement scheme

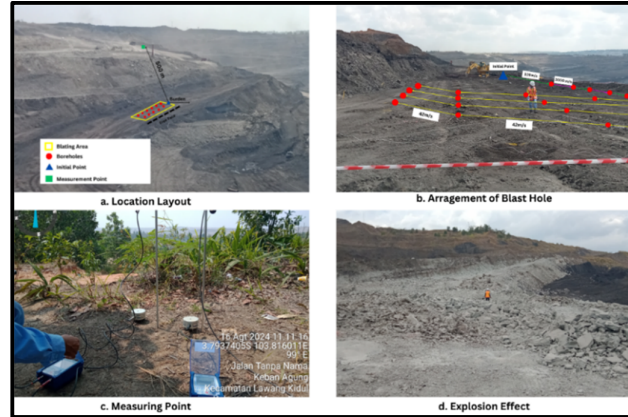


Figure 7. Blasting acoustic measurement setting and measurement area

**2.4. Existing Noise Regulation and Damage Prevention Criteria**

Indonesian mining operations are governed by a multi-layered regulation aimed at supporting environmental protection as well as occupational safety. Various national regulations and ministerial decrees specify permissible limits for noise and airblast. A distinction should be made between regulations governing general ambient noise, measured on the A-weighted decibel scale (dBA), and those governing impulsive air overpressure caused by blasting, measured on the linear decibel scale (dBL). The dBA scale is frequency weighted to mimic the human ear and is used for continuous noise sources, while the dBL scale is a flat response and is required to accurately determine the peak pressure of transient events such as blasts.

The most directly relevant standard for this study is SNI 7570:2023, a revision of SNI 7570:2010, which regulates noise levels in mining activities, including those generated by blasting. This standard establishes methods for noise measurement, the equipment used, and the interpretation of measurement results to ensure that noise levels produced by blasting do not exceed specified limits. High-pressure air blasting often generates significant noise; therefore, this regulation can serve as a basis for monitoring the acoustic impact of blasting.

Various regulations in Indonesia govern noise standards and environmental impacts associated

with mining activities, particularly during blasting operations. The Minister of Environment's Decree Number 48 of 1996 establishes maximum noise limits in dBA units according to the area type, with limits ranging from 55 dBA for residential areas to 70 dBA for industrial areas. This regulation requires companies to report noise monitoring results periodically.

The Minister of Energy and Mineral Resources (ESDM) Decision Number 1827 K/30/MEM/2018 regulates safety aspects and the management of air blasts caused by blasting. Mining companies are required to design and monitor air pressure during blasting, as well as implement appropriate blasting designs to ensure personnel and environmental safety. This differs from Government Regulation Number 55 of 2010, which emphasizes government supervision and guidance regarding workplace safety in the mining sector.

SNI 7571:2010 focuses on measuring the impact of ground vibrations from blasting to prevent damage to nearby building structures. Meanwhile, SNI 7570:2023 regulates measurement methods and noise limits in mining activities, including noise caused by air blasts, with a maximum limit of 120 dBL.

The Minister of Defense Regulation Number 5 of 2016 regulates the management of explosives in terms of storage and distribution, which directly impacts the control of air blasts in mining. Unlike

other regulations, this rule focuses more on the security aspects of explosives.

Overall, although these regulations have different focuses, they all contribute to environmental management and workplace safety in mining areas. The latest standards, such as SNI 7570:2023, provide more technical guidance on noise measurement in the mining sector to ensure operations remain within safe limits and do not disturb the surrounding environment.

### 3. Results and Discussion

#### 3.1. Overview of Data and Analytical Framework

The data set analyzed, shown in Table 2, comprises 30 blasting sites characterized by their frequency, dBA, and dBL levels measured, as well as the corresponding predictions made using various acoustic prediction models. These models encompass a range of approaches, including analytical equations based on the scaled-distance concept, the Finn correction-derived equation, and site-specific regression models. Their performance must first be understood by identifying the physical processes they aim to represent.

Blast-induced air overpressure is a complex physical effect caused by the detonation of explosives. The heat is released very quickly through an exothermic chemical reaction, generating a tremendous volume of high-pressure, superheated gas that violently explodes, pushing the surrounding air outward and emitting a pressure wave spherically from the source [43]. The wave, also called a blast wave, is one where pressure rapidly increases at the wave front from ambient to a maximum value, then decreases nearly exponentially back to ambient pressure, followed by a negative pressure phase before equilibrium is restored. The part of this pressure wave that is audible, typically corresponding to a frequency greater than 20 Hz, is perceived as noise [44]. The Finn equation model was derived from regression analysis based on measured data and A-correction data, as governed by Finn [26], as shown in Table 3. This A-correction is referenced in Standard Nasional Indonesia (SNI) 7570:2023 for converting the dBL value to dBA. Additionally, a separate regression model based on the measured

dBA values was included to provide a more conservative estimation framework. Three other predictive models were also employed, each originating from previous well-established studies. These models are all implementations of the scaled-distance concept, a foundation of blast impact prediction. This concept uses the Hopkinson-Cranz scaling law, which refers to a fundamental scaling law in explosives engineering, used to predict the effects of an explosion at different distances and charge weights. Various explosive energy yield blasts ( $W$ ) will create self-similar pressure waves at the same scaled distances ( $Z = \frac{D}{W^{1/3}}$ ), where  $D$  is the distance from the source. The logarithmic form of these equations includes the geometric spreading and attenuation of the blast wave.

The first prediction model was proposed by ONECRC [10], as follows:

$$dB(A) = -16,02 \log\left(\frac{D}{W^{1/3}}\right) + 97,46 \quad (1)$$

Here,  $W$  denotes the maximum charge per delay (kg/delay), and  $D$  represents the distance from the source (m). The second model, proposed by IOERSNU [12], is expressed as:

$$dB(A) = -14,05 \log\left(\frac{D}{W^{1/3}}\right) + 97,46 \quad (2)$$

Where  $W$  represents the maximum charge per delay (kg/delay), and  $D$  stands for the distance (m) from the source. The third noise prediction equation developed by Yang and Kim [11] is shown below:

$$dB(A) = -14 \log\left(\frac{D}{W^{1/3}}\right) + 88,1 \quad (3)$$

In each of these equation models predict the expected dBA values as a function of variables, including frequency, scale distance, delay, charge per delay, and hole configuration. The measured data revealed a mean dBA of approximately 60.7 dB, with a range of 50.4 to 68.6 dB. The measured dBL average was 112.3 dB, indicating the intense nature of explosive blasts, albeit with significant attenuation of audible (A-weighted) sound levels. A high positive relationship (Pearson's  $r \approx 0.87$ ) existed between dBA and dBL measures.

**Table 2. Measured results of dBA and dBL values as well as dBA prediction by various prediction models**

| No | F     | dBA Meas. | dBL Meas. | W    | dBA Prediction By Finn |           |           | dBA Prediction by Regr. |           | dBA Prediction by Eq.1 |          | dBA Prediction by Eq 2 |          | dBA Prediction by Eq 3 |          |
|----|-------|-----------|-----------|------|------------------------|-----------|-----------|-------------------------|-----------|------------------------|----------|------------------------|----------|------------------------|----------|
|    |       |           |           |      | A Correction           | dBA Calc. | Error (%) | dBA Calc.               | Error (%) | dBA Calc.              | Error(%) | dBA Calc.              | Error(%) | dBA Calc.              | Error(%) |
|    |       |           |           |      | 1                      | 2.6       | 65.6      | 118.4                   | 264       | -90.937                | 27.463   | 138.866                | 64.222   | 2.146                  | 67.154   |
| 2  | 12.8  | 56.8      | 113.5     | 264  | -64.375                | 49.125    | 15.624    | 60.323                  | 5.840     | 67.154                 | 15.418   | 70.881                 | 19.865   | 65.399                 | 13.148   |
| 3  | 6.55  | 63.6      | 112.5     | 345  | -79.631                | 32.869    | 93.497    | 59.527                  | 6.842     | 67.774                 | 6.159    | 71.425                 | 10.955   | 65.864                 | 3.437    |
| 4  | 8.9   | 63.2      | 112.9     | 270  | -73.516                | 39.384    | 60.473    | 59.846                  | 5.605     | 67.206                 | 5.961    | 70.926                 | 10.893   | 65.438                 | 3.420    |
| 5  | 6.85  | 62.5      | 120.8     | 280  | -78.825                | 41.975    | 48.899    | 66.132                  | 5.491     | 67.290                 | 7.119    | 71.000                 | 11.972   | 65.501                 | 4.582    |
| 6  | 9.85  | 59.8      | 116.5     | 460  | -71.174                | 45.326    | 31.933    | 62.710                  | 4.640     | 68.442                 | 12.626   | 72.010                 | 16.956   | 66.363                 | 9.890    |
| 7  | 12.35 | 57.1      | 108.4     | 299  | -65.366                | 43.034    | 32.686    | 56.265                  | 1.484     | 67.443                 | 15.335   | 71.134                 | 19.729   | 65.615                 | 12.977   |
| 8  | 12.8  | 58.6      | 107.5     | 184  | -64.375                | 43.125    | 35.885    | 55.549                  | 5.493     | 66.317                 | 11.636   | 70.146                 | 16.460   | 64.772                 | 9.528    |
| 9  | 4.3   | 66.2      | 111.5     | 216  | -85.913                | 25.587    | 158.727   | 58.732                  | 12.716    | 66.688                 | 0.732    | 70.472                 | 6.063    | 65.050                 | 1.768    |
| 10 | 5.1   | 65.2      | 117.9     | 448  | -83.632                | 34.268    | 90.263    | 63.824                  | 2.156     | 68.380                 | 4.651    | 71.956                 | 9.389    | 66.317                 | 1.685    |
| 11 | 5.9   | 62.2      | 112.4     | 280  | -81.403                | 30.997    | 100.665   | 59.448                  | 4.630     | 67.290                 | 7.565    | 71.000                 | 12.395   | 65.501                 | 5.040    |
| 12 | 5.95  | 63.9      | 120.7     | 224  | -81.266                | 39.434    | 62.041    | 66.052                  | 3.258     | 66.773                 | 4.302    | 70.546                 | 9.421    | 65.113                 | 1.863    |
| 13 | 9.85  | 59.8      | 110.3     | 280  | -71.174                | 39.126    | 52.840    | 57.777                  | 3.502     | 67.290                 | 11.131   | 71.000                 | 15.775   | 65.501                 | 8.704    |
| 14 | 10.55 | 58.2      | 105.5     | 280  | -69.496                | 36.004    | 61.648    | 53.957                  | 7.863     | 67.290                 | 13.509   | 71.000                 | 18.029   | 65.501                 | 11.146   |
| 15 | 11    | 59.2      | 110.7     | 280  | -68.438                | 42.262    | 40.079    | 58.095                  | 1.902     | 67.290                 | 12.023   | 71.000                 | 16.620   | 65.501                 | 9.620    |
| 16 | 11.25 | 57.1      | 106.2     | 280  | -67.858                | 38.342    | 48.922    | 54.514                  | 4.743     | 67.290                 | 15.144   | 71.000                 | 19.578   | 65.501                 | 12.826   |
| 17 | 11.5  | 59.5      | 113.2     | 280  | -67.283                | 45.917    | 29.581    | 60.084                  | 0.972     | 67.290                 | 11.577   | 71.000                 | 16.198   | 65.501                 | 9.162    |
| 18 | 12.05 | 59.9      | 112.6     | 280  | -66.036                | 46.564    | 28.639    | 59.607                  | 0.492     | 67.290                 | 10.983   | 71.000                 | 15.634   | 65.501                 | 8.551    |
| 19 | 3.65  | 66.2      | 120.4     | 540  | -87.806                | 32.594    | 103.104   | 65.813                  | 0.588     | 68.813                 | 3.798    | 72.336                 | 8.483    | 66.642                 | 0.663    |
| 20 | 5.9   | 65        | 109.5     | 270  | -81.403                | 28.097    | 131.342   | 57.140                  | 13.755    | 67.206                 | 3.282    | 70.926                 | 8.356    | 65.438                 | 0.669    |
| 21 | 7     | 64.2      | 124       | 420  | -78.425                | 45.575    | 40.867    | 68.678                  | 6.520     | 68.231                 | 5.907    | 71.825                 | 10.616   | 66.205                 | 3.029    |
| 22 | 5.1   | 64.6      | 114       | 550  | -83.632                | 30.368    | 112.722   | 60.721                  | 6.389     | 68.856                 | 6.181    | 72.374                 | 10.741   | 66.674                 | 3.110    |
| 23 | 3.85  | 66.4      | 122.6     | 1026 | -87.220                | 35.380    | 87.676    | 67.564                  | 1.723     | 70.302                 | 5.550    | 73.642                 | 9.834    | 67.757                 | 2.003    |
| 24 | 1.85  | 68.6      | 115.6     | 715  | -93.229                | 22.371    | 206.649   | 61.994                  | 10.656    | 69.464                 | 1.245    | 72.907                 | 5.908    | 67.130                 | 2.190    |
| 25 | 7.75  | 51.9      | 106.2     | 392  | -76.452                | 29.748    | 74.464    | 54.514                  | 4.796     | 68.071                 | 23.756   | 71.685                 | 27.600   | 66.086                 | 21.465   |
| 26 | 2.65  | 50.4      | 105.7     | 392  | -90.786                | 14.914    | 237.932   | 54.116                  | 6.868     | 68.071                 | 25.959   | 71.685                 | 29.692   | 66.086                 | 23.735   |
| 27 | 2.75  | 51.5      | 104       | 392  | -90.484                | 13.516    | 281.031   | 52.764                  | 2.395     | 68.071                 | 24.343   | 71.685                 | 28.158   | 66.086                 | 22.071   |
| 28 | 9.15  | 50.5      | 105.4     | 392  | -72.893                | 32.507    | 55.350    | 53.878                  | 6.269     | 68.071                 | 25.812   | 71.685                 | 29.553   | 66.086                 | 23.584   |
| 29 | 9.75  | 50.8      | 107.2     | 392  | -71.417                | 35.783    | 41.967    | 55.310                  | 8.154     | 68.071                 | 25.372   | 71.685                 | 29.134   | 66.086                 | 23.130   |
| 30 | 9.95  | 51.8      | 106.1     | 392  | -70.932                | 35.168    | 47.292    | 54.435                  | 4.840     | 68.071                 | 23.903   | 71.685                 | 27.739   | 66.086                 | 21.617   |

**Table 3. A-weighting response**

| Frequency (Hz) | A-weighting (dB) |
|----------------|------------------|
| 8              | -77.8            |
| 10             | -70.4            |
| 12.5           | -63.4            |
| 16             | -56.7            |
| 20             | -50.5            |
| 25             | -44.7            |
| 31.5           | -39.4            |
| 40             | -34.6            |
| 50             | -30.2            |
| 63             | -26.2            |
| 80             | -22.5            |
| 100            | -19.1            |
| 125            | -16.1            |
| 160            | -13.4            |
| 200            | -10.9            |
| 250            | -8.6             |
| 315            | -6.6             |
| 400            | -4.8             |
| 500            | -3.2             |
| 630            | -1.9             |
| 800            | -0.8             |
| 1000           | 0                |
| 1250           | 0.6              |
| 1600           | 1                |
| 2000           | 1.2              |
| 2500           | 1.3              |
| 3150           | 1.2              |
| 4000           | 1                |
| 5000           | 0.5              |
| 6300           | -0.1             |
| 8000           | -1.1             |
| 10000          | -2.5             |
| 12500          | -4.3             |
| 16000          | -6.6             |
| 20000          | -9.3             |

**3.2. Comparative Accuracy of Predictive Equations**

To assess model accuracy, the absolute percentage error was calculated between measured and model-predicted dBA values. The analysis points out important disadvantages in the application of generalized analytical and empirical models and indicates the necessity for site-specific calibration. The Finn equation, although widely used in mining acoustics modeling, especially in Indonesia, exhibits inferior prediction performance, with an average error of 86% and a maximum error exceeding 280%. This discrepancy suggests a systemic inconsistency between the model's assumptions and the acoustic profiles observed in the study's operational environment. This profound unreliability is a consequence of the empirical models' inherent limitations, which puts them under a non-generalizable nature [13]. The models consist of a function of site constant that integrates the combined, interactive effects of numerous variables besides charge mass and distance, including blast design such as stemming height, burden, face orientation, geology, and topographic shielding [45]. The constant also implicitly includes the meteorological conditions under which the original calibration data were made. Meteorological factors like wind speed, wind direction, and temperature gradients may considerably influence the sound propagation by

refraction and thus cause a significant increase or decrease of noise levels with distance. Applying an empirical formula to a new location without recalibration is therefore scientifically uncertain. The gross discrepancies observed here justify that the implicit assumptions incorporated into the Finn equation coefficients are inherently unsuitable for the propagation condition of this current research area.

However, the equations (Eqs. 1, 2, and 3) yielded improving results, with mean errors of 11%, 16%, and 9%, respectively. Of these, Equation 3 was the most reliable model, with an extremely low error of 0% to a maximum error of 24%. This finding showed that a Korean experiment concluded that the most in agreement with their field data measurements was the ONECRC equation (Eq. 1) [2]. The present research, on the other hand, rates the Yang and Kim model as superior. This provides clear evidence of the fact that the comparative accuracy of generalized analytical and empirical models largely depends on the similarity of the new location of application with the conditions under which the model was initially developed. The performance of analytical and empirical models depends on the context, which enables thorough pre-site testing or selection based on models developed under the same geological and operational conditions.

The measurement-based correction model, or the regression-derived equation based on the measured data, performed best overall, with an average error of only 5%. It is consistent with empirical sound modeling best practices, which involve using site-specific correction factors to account for terrain, meteorological, and structural factors [46,47]. Advanced predictive models used in regulatory and planning contexts, such as the US Army's UNAPS models, in fact rely on this principle, requiring precise local information to predict [48]. The improved performance of our site-specific calibrated model thus constitutes an internal test of this principle, with the outcome that even a simple regression model will perform dramatically better than uncalibrated, generalized equations.

These values are illustrated in the boxplot shown in **Figure 8**, which represents the spread of absolute errors across the predictive equation models. The measured corrections-based model also has a small interquartile range and little occurrence of outliers, as seen to affirm its stability. Scatter plots in **Figure 9** subsequently illustrate that Equation 3 and the measurement-based

correction through the regression equation model also closely follow the 1:1 line of ideal prediction.

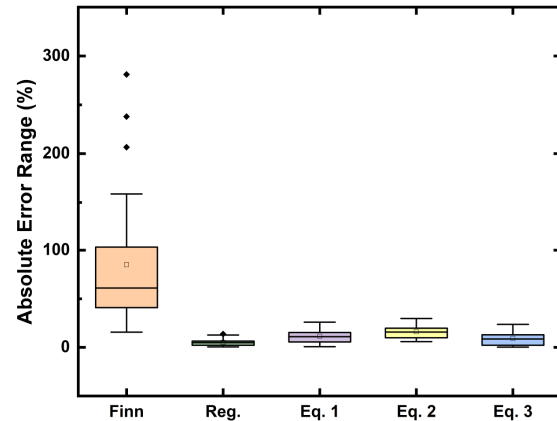


**Figure 8. Absolute error comparison across predictive equation models.**

### 3.3. Machine Learning Predictive Modeling

The constraints of the empirical model, especially its inability to elaborate complex, non-linear relationships among various influencing parameters, have prompted the need for more advanced data-driven approaches [49]. The increasing deployment of machine learning (ML) techniques has enabled more accurate, efficient, and scalable predictions. Recent literature indicates that ML algorithms such as Random Forest (RF), Artificial Neural Networks (ANN), Support Vector Machines (SVM), and other ensemble and hybrid models predict the effects of blast-induced air overpressure and ground vibration with consistently higher precision than standard empirical methods [13].

Guo et al. [50] employed a Random Forest model to predict railway-induced vibrations, particularly in high-speed rail (HSR) systems. Complementing this approach, Yao and Fang [51] developed a methodology combining numerical simulation with Random Forest-based predictive modeling, allowing them to evaluate the influence of factors such as train speed, axle load, and soil characteristics on structural vibrations. Cao et al. [52] further advanced machine learning-based railway vibration analysis through a comparative evaluation of multiple algorithms, including Linear Regression, Support Vector Machines, and Random Forest.

In the context of blasting-induced vibrations, Yan et al. [53] conducted an extensive study comparing six machine learning algorithms, including Random Forest, K-Nearest Neighbors, Artificial Neural Networks, and Support Vector

Regression, as well as hybrid models optimized via the Arithmetic Optimization Algorithm, to investigate peak particle velocity (PPV). The study reported that the machine learning-developed model achieved superior predictive accuracy. Overall, machine learning can potentially develop models that offer significant improvements in predictive accuracy, robustness to noise, and adaptability to complex systems compared to traditional empirical or numerical methods.

Here, we investigate the predictive model by utilizing Random Forest and Artificial Neural Network to calculate the dBA value from the frequency and dBL measured in RStudio. The predicted dBA values obtained using Random Forest and Artificial Neural Network in RStudio are presented in Table 4. The RF model

demonstrated superior performance in terms of consistency and robustness across different frequencies and dBL levels. Quantitatively, both models produced average percentage errors of approximately 2%; however, the RF model showed a closer residual grouping around zero and a lower standard deviation in error rates. Most predictions by the RF model fell within the error range of 0% to 3%, with only a few cases exceeding 5%. In contrast, the ANN model exhibited greater variability, with error rates reaching up to 10–11%. These anomalies were particularly observed in mid-frequency ranges (for example, 9.75 Hz and 10.55 Hz), where the dBA values were significantly overestimated or underestimated by the ANN model.

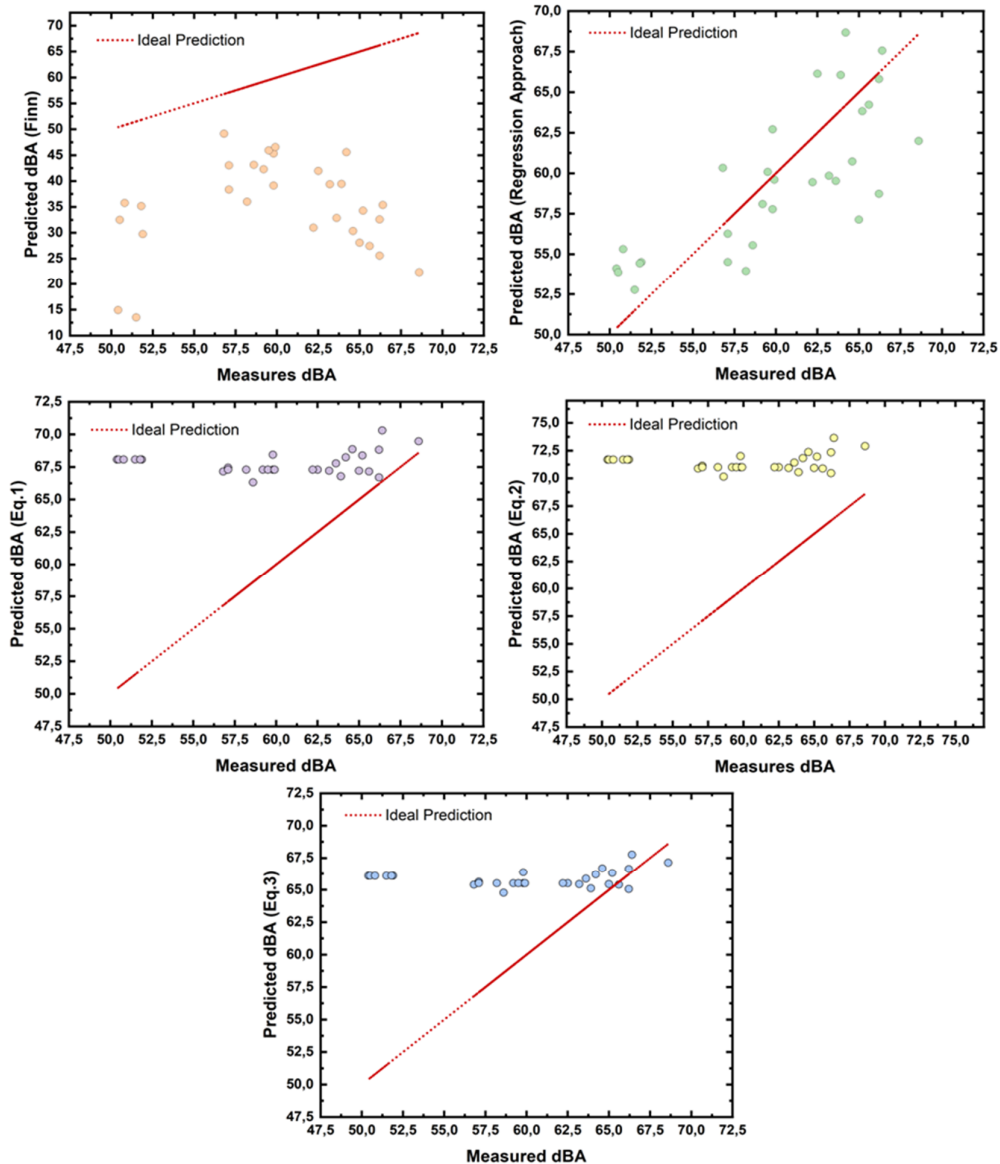


Figure 9. Predicted dBA derived by various equation models against the ideal predicted dBA

**Table 4. Comparison of machine learning predicted dBA values derived from the measured frequency and dBL**

| No | F     | dBA Meas. | dBL Meas. | Predicted dBA by RF |           | Predicted dBA by ANN |           |
|----|-------|-----------|-----------|---------------------|-----------|----------------------|-----------|
|    |       |           |           | dBA Calc.           | Error (%) | dBA Calc.            | Error (%) |
| 1  | 2.6   | 65.6      | 118.4     | 64.466              | 2         | 67.269               | 2         |
| 2  | 12.8  | 56.8      | 113.5     | 58.455              | 3         | 58.257               | 3         |
| 3  | 6.55  | 63.6      | 112.5     | 63.412              | 0         | 63.156               | 1         |
| 4  | 8.9   | 63.2      | 112.9     | 60.982              | 4         | 60.972               | 4         |
| 5  | 6.85  | 62.5      | 120.8     | 63.517              | 2         | 63.493               | 2         |
| 6  | 9.85  | 59.8      | 116.5     | 59.900              | 0         | 60.487               | 1         |
| 7  | 12.35 | 57.1      | 108.4     | 57.730              | 1         | 57.943               | 1         |
| 8  | 12.8  | 58.6      | 107.5     | 57.330              | 2         | 57.465               | 2         |
| 9  | 4.3   | 66.2      | 111.5     | 65.165              | 2         | 64.782               | 2         |
| 10 | 5.1   | 65.2      | 117.9     | 65.059              | 0         | 65.026               | 0         |
| 11 | 5.9   | 62.2      | 112.4     | 63.411              | 2         | 63.772               | 2         |
| 12 | 5.95  | 63.9      | 120.7     | 63.909              | 0         | 64.313               | 1         |
| 13 | 9.85  | 59.8      | 110.3     | 59.575              | 0         | 59.819               | 0         |
| 14 | 10.55 | 58.2      | 105.5     | 55.288              | 5         | 53.116               | 10        |
| 15 | 11    | 59.2      | 110.7     | 59.538              | 1         | 59.087               | 0         |
| 16 | 11.25 | 57.1      | 106.2     | 55.877              | 2         | 55.806               | 2         |
| 17 | 11.5  | 59.5      | 113.2     | 59.375              | 0         | 58.991               | 1         |
| 18 | 12.05 | 59.9      | 112.6     | 59.508              | 1         | 58.606               | 2         |
| 19 | 3.65  | 66.2      | 120.4     | 65.645              | 1         | 66.337               | 0         |
| 20 | 5.9   | 65        | 109.5     | 63.679              | 2         | 61.684               | 5         |
| 21 | 7     | 64.2      | 124       | 63.847              | 1         | 63.471               | 1         |
| 22 | 5.1   | 64.6      | 114       | 64.527              | 0         | 64.805               | 0         |
| 23 | 3.85  | 66.4      | 122.6     | 65.431              | 1         | 66.109               | 0         |
| 24 | 1.85  | 68.6      | 115.6     | 65.085              | 5         | 67.896               | 1         |
| 25 | 7.75  | 51.9      | 106.2     | 53.363              | 3         | 52.619               | 1         |
| 26 | 2.65  | 50.4      | 105.7     | 53.137              | 5         | 51.311               | 2         |
| 27 | 2.75  | 51.5      | 104       | 53.211              | 3         | 50.827               | 1         |
| 28 | 9.15  | 50.5      | 105.4     | 52.253              | 3         | 51.087               | 1         |
| 29 | 9.75  | 50.8      | 107.2     | 53.503              | 5         | 57.345               | 11        |
| 30 | 9.95  | 51.8      | 106.1     | 52.986              | 2         | 54.531               | 5         |

Figure 10 depicts a comparison of observed and predicted dBA values for both models. The RF model is consistently accurate, exhibiting minimal deviations from the actual measurements. On the other hand, the ANN predictions exhibited more pronounced fluctuations, particularly in the lower dBA range (~50 dBA), suggesting sensitivity to input variability and potential overfitting. Boxplot analysis in Figure 11 further highlighted the advantage of the RF model, as it showed a narrower interquartile range and fewer outliers than the ANN model. This demonstrates a more stable distribution of errors, which is crucial for practical applications in noise impact assessment.

Additional insights into the models' behaviors across the acoustic spectrum are shown in Figure 12a. The RF model maintained relatively stable error margins across all frequency bands, whereas the ANN model's errors were more erratic, especially in the range of 8–12 Hz. This variability can be attributed to the inherent complexity of the ANN structure, which, while theoretically capable of performing more efficient nonlinear modeling,

requires more sophisticated tuning and training data to achieve optimal performance. As an ensemble algorithm, RF mitigates overfitting risk through the averaging of predictions from several decorrelated decision trees. This design is inherently robust and particularly effective for small datasets, where a single complex model might struggle to generalize [54]. In contrast, although ANNs are recognized as superior in approximating a wide range of functions, they tend to have higher variance in most cases. This characteristic can cause their performance to fluctuate, resulting in less stability compared to other models in certain contexts. Their behavior exhibits high sensitivity to numerous factors, including the specific network architecture, hyperparameter selection, and the dimensions and representativeness of the training data. All these factors greatly influence the overall performance and effectiveness of the model [55]. The findings indicate that, for this particular dataset (n=30), the ensemble characteristics of RF provide a more stable outcome. The ANN, with greater flexibility,

is more demanding in terms of data requirements. This suggests that RF would be more suitable when data are limited, as it offers stable predictions without sacrificing reliability.

Figures 12b and 12c illustrate the relationship between prediction error and predicted dBA, providing further evidence of the models' efficacy. For the RF model, the residuals were uniformly

distributed around the zero-error line, indicating minimal systematic bias. Conversely, the ANN model displayed a more dispersed residual pattern, with some data points deviating significantly from the zero-error line. This dispersion suggests that the ANN model may be less reliable for applications requiring high-precision predictions, such as real-time noise monitoring and regulatory reporting.

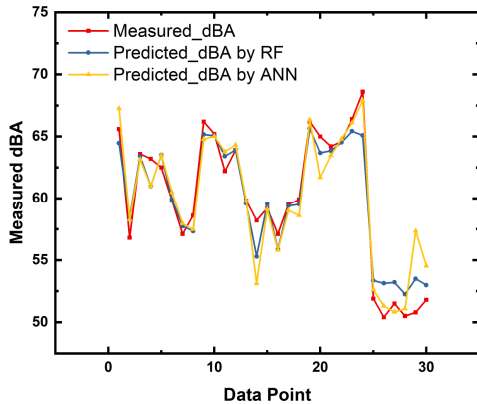


Figure 10. The measured vs. predicted dBA for both the Random Forest (RF) and Artificial Neural Network (ANN) models

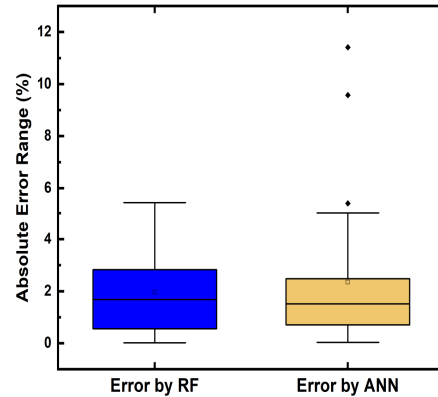


Figure 11. Absolute error comparison between RF and ANN

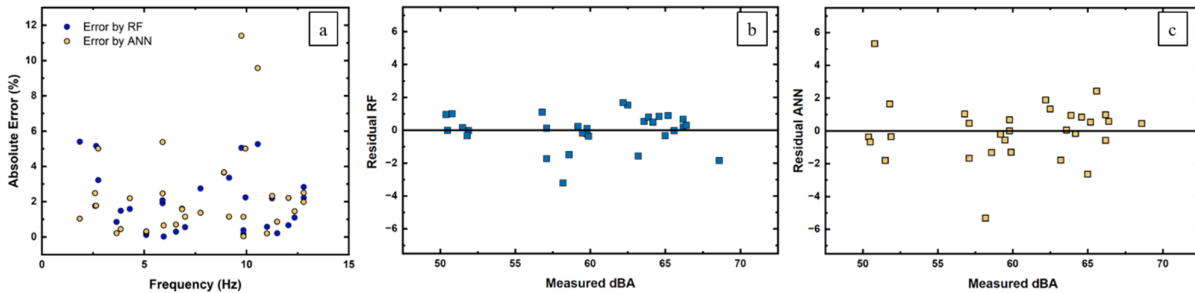


Figure 12. a) Absolute error behaviour of RF and ANN model across the frequency; b) Residual plot of RF model as a function of measured dBA; c) Residual plot of ANN model as a function of measured dBA

Most ML studies for blast prediction utilize blast design factors, including charge weight, burden, spacing, and stemming, as well as rock mass factors, to predict outcome measures such as air overpressure or ground vibration [13]. In contrast, the models in this study use observed acoustic data (dBL and frequency) to predict another acoustic factor, dBA. The models demonstrate a paradigm for addressing hardware limitations and provide a reliable method for deriving dBA from dBL measurements for regulatory compliance.

### 3.4. The Challenge of Balancing Understandability and Precision

This study underscores a significant challenge in the application of predictive modeling in the

context of regulated environmental areas. This challenge revolves around the delicate balance between keeping the model interpretable and achieving high predictive precision. Finding a balance between these two needs is essential as stakeholders need to trust and understand the models and, at the same time, be able to appreciate the accuracy of predictive capabilities.

In mine sites, where multiple sources of noise dynamically interact with each other and climatic conditions change throughout the day, it is necessary to use prediction models that are adaptive to changes in noise while maintaining low error levels. Machine learning models like RF satisfy this condition owing to their ensemble nature and resistance to overfitting, especially when trained with diverse datasets. ANN models, with their best architecture and noise

regularization, are also promising but require larger training sets to offset their higher variance.

However, the interpretability of machine learning models remains less than that of analytical equations; therefore, perhaps the best approach would be a hybrid model where machine learning complements and does not replace physically based prediction models for engineering applications. This interpretability is not merely a theoretical benefit but has practical, regulatory, and scientific implications that sustain the continued relevance of these models in noise prediction, environmental impact assessment, and land-use planning in post-mining contexts.

Analytical or physically based models are constructed on the foundation of established physical principles. This clarity provides an invaluable degree of transparency. When a prediction is made using such a model, practitioners can easily trace the output back through the contributing factors, understanding exactly how changes in environmental conditions or source characteristics influence the result. This level of transparency contrasts sharply with data-driven models, particularly deep learning architectures, which often function as "black boxes." In these models, the relationship between input features and output predictions is encoded within complex, multi-layered networks whose internal workings are not intuitively accessible.

Interpretability may also play a critical role in regulatory and legal frameworks. Environmental impact assessment standards typically require that any model used for impact prediction be transparent, traceable, and justifiable. Physically based models fulfill these criteria inherently, as their structure and assumptions are clearly defined and scientifically validated. Each input, such as a blasting parameter, is measurable, and its impact on the output is logically derivable. This traceability ensures that model outputs can be defended in legal contexts and trusted by regulatory bodies—an advantage that is crucial when compliance is at stake or when environmental assessments are subjected to public or judicial scrutiny.

The future of blast impact modeling does not lie in the choice between two extremes but in the development of hybrid frameworks that include the strengths of both. One such exciting direction is collaboration with Explainable AI (XAI) techniques. For instance, it is feasible to use after techniques such as Shapley Additive Explanations (SHAP) on black-box models. These strategies quantify the contribution of every input factor to a

prediction and provide transparency without sacrificing the predictive power of the model [13].

There exists a more integrated strategy in the new discipline of Physics-Informed Machine Learning (PIML). For example, Physics-Informed Neural Networks (PINNs) incorporate governing physical equations like acoustic wave propagation equations into the model loss function during training [56]. This constraint guarantees that the model generates solutions in line with both training data and fundamental physical principles. By combining machine learning's data-fitting capability with the theoretical consistency of physics-based modeling, these hybrid approaches represent the next frontier in modeling, providing not just highly accurate solutions but more trustworthy and interpretable.

A number of practical recommendations follow from these findings. First, mining operations should strive to use locally calibrated, measurement-based dBA estimation models. This method yields more precise results, thereby enhancing the reliability of environmental impact statements. Second, in cases where data conditions permit, the inclusion of Random Forest or similar machine learning models can provide greater predictive accuracy, especially in complex acoustic environments. Third, practitioners need to exercise caution when applying outdated models, such as the Finn equation, particularly in sensitive zones or in rigorous regulatory regimes with stringent decibel ceilings.

#### 4. Conclusions

This study develops a novel strategic framework for acoustic assessment due to mining activity by systematically comparing the performance of machine learning, analytical, and measurement models. Our findings highlight the significant trade-off between the predictive capabilities of advanced algorithms and the engineering need for model interpretability.

RF emerged as the most accurate and consistent, with an average error of 2% and minimal deviation across frequencies and sound levels. Its robustness and adaptability make it highly suitable for real-time environmental monitoring. In contrast, the ANN model, while capable of modeling complex nonlinearities, exhibited higher error variability and was less reliable, particularly in low dBA conditions. Finn's model, despite its theoretical basis, produced frequent implausible outputs.

Among the analytical approaches, Equation 3 (Eq.3) achieves competitive accuracy with the

added benefits of interpretability and low computational demand. Such a combination of features is well suited as an evaluation method for regulatory compliance. Although the measurement-derived equation shows the lowest error, Eq. 3 provides a pragmatic balance between physical interpretability and numerical precision, making it a strong candidate for compliance assessments or use in environments with constrained computational infrastructure.

This framework has important benefits for smart mining operations. It reduces noise and increases worker safety. From an environmental management perspective, it provides excellent tools for conducting Environmental Impact Assessments by ensuring compliance with regulations. Finally, this research provides an outlook on practical methods to select the most appropriate predictive model for technical, operational, and regulatory requirements in mining.

## References

- [1]. Chi, M.-b., Li, Q.-s., Cao, Z.-g., Fang, J., Wu, B.-y., Zhang, Y., Wei, S.-r., Liu, X.-q., Yang, Y.-m. (2022). Evaluation of water resources carrying capacity in ecologically fragile mining areas under the influence of underground reservoirs in coal mines. *Journal of Cleaner Production*, 379, 134449
- [2]. Lee, C.-W., Kim, J., & Kang, G.-C. (2018). Full-Scale Tests for Assessing Blasting-Induced Vibration and Noise. *Shock and Vibration*, 2018(1), 9354349
- [3]. Karagianni, A., Lazos, I., & Chatzipetros, A. (2018). Remote Sensing Techniques in Disaster Management: Amynteon Mine Landslides, Greece. *Int. Arch. Photogramm. Remote Sens. Spatial Inf. Sci.*, XLII-3/W4, 269-276
- [4]. Hilson, G. (2019). Why is there a large-scale mining 'bias' in sub-Saharan Africa?. *Land Use Policy*, 81, 852-861.
- [5]. Tiwari, S. K., Kumaraswamidhas, L. A., & Garg, N. (2023). Assessment of noise pollution and associated subjective health complaints in Jharia Coalfield, India: A structural equation model analysis. *Noise Mapping*, 10(1)
- [6]. Mocek, P. (2020). Noise in the Mining Work Environment - Causes, Effects and Threats. *IOP Conference Series: Earth and Environmental Science*, 609(1), 012075
- [7]. Baffoe, P. E., Duker, A. A., & Senkyire-Kwarteng, E. V. (2022). Assessment of health impacts of noise pollution in the Tarkwa Mining Community of Ghana using noise mapping techniques. *Global Health Journal*, 6(1), 19-29
- [8]. Waye, K. P. (2011). Effects of Low Frequency Noise and Vibrations: Environmental and Occupational Perspectives. *Encyclopedia of Environmental Health*, 240 -253.
- [9]. David E. Siskind, V. J. S., Mark S. Stagg, John W. Kopp (1980). Structure Response and Damage Produced by Airblast From Surface Mining. *Report of Investigations 8485, United States Department of The Interior, Bureau of Mines*
- [10]. ONECRC (1997). A study on examining criteria on cause and effect relationship for noise damage and calculation of damage cost. *South Korea: Office of National Environmental Conflict Resolution Commission*
- [11]. Yang Hyung-sik, K. N.-s. Blasting design considering noise and vibration regulatory law, *KSRM annual conference of Conference*, 7
- [12]. IOERSNU (2000). Influence evaluation of blasting-induced vibration and noise at rock excavation part of 9th construction area of Daegu-Pohang Expressway. *Institute of Engineering Research at Seoul National University*
- [13]. Dumakor-Dupey, N. K., Arya, S., & Jha, A. (2021). Advances in Blast-Induced Impact Prediction—A Review of Machine Learning Applications. *Minerals*, 11(6), 601
- [14]. Victor Amoako Temeng, Y. Y. Z., Clement Kweku Arthur (2021). Blast-Induced Noise Level Prediction Model Based on Brain Inspired Emotional Neural Network. *Journal of Sustainable Mining*, 20(1), 12
- [15]. Jahed Armaghani, D., Hajihassani, M., Sohaei, H., Tonnizam Mohamad, E., Marto, A., Motaghedi, H., et al. (2015). Neuro-fuzzy technique to predict air-overpressure induced by blasting. *Arabian Journal of Geosciences*, 8(12), 10937-10950
- [16]. Jahed Armaghani, D., Hasanipanah, M., & Tonnizam Mohamad, E. (2016). A combination of the ICA-ANN model to predict air-overpressure resulting from blasting. *Engineering with Computers*, 32(1), 155-171
- [17]. Jahed Armaghani, D., Hasanipanah, M., Mahdiyar, A., Abd Majid, M. Z., Bakhshandeh Amnieh, H., & Tahir, M. M. D. (2018). Airblast prediction through a hybrid genetic algorithm-ANN model. *Neural Computing and Applications*, 29(9), 619-629
- [18]. Jahed Armaghani, D., Hajihassani, M., Marto, A., Shirani Faradonbeh, R., & Mohamad, E. T. (2015). Prediction of blast-induced air overpressure: a hybrid AI-based predictive model. *Environmental Monitoring and Assessment*, 187(11), 666
- [19]. Bui, X.-N., Nguyen, H., Le, H.-A., Bui, H.-B., & Do, N.-H. (2020). Prediction of Blast-induced Air Overpressure in Open-Pit Mine: Assessment of Different Artificial Intelligence Techniques. *Natural Resources Research*, 29(2), 571-591

- [20]. Wen, P.-J., & Huang, C. (2020). Noise Prediction Using Machine Learning with Measurements Analysis. *Applied Sciences*, 10(18), 6619
- [21]. Yang, Y., Hou, K., Sun, H., Guo, L., & Zhe, Y. (2025). Random Forest-Based Stability Prediction Modeling of Closed Wall for Goaf. *Applied Sciences*, 15(5), 2300
- [22]. Chi, X., Yue, Y., Jin, Z., Zhang, P., & Sun, X. (2025). PSO-SVM Machine Learning for Blasting Vibration Velocity Prediction in Open Pit Mines. *Preprints*, 2025031679
- [23]. Kazemi, M. M. K., Nabavi, Z., & Khandelwal, M. (2023). Prediction of blast-induced air overpressure using a hybrid machine learning model and gene expression programming (GEP): A case study from an iron ore mine. *AIMS Geosciences*, 9(2), 357-381.
- [24]. Peterson, R. A., McGrath, M., & Cavanaugh, J. E. (2024). Can a Transparent Machine Learning Algorithm Predict Better than Its Black Box Counterparts? A Benchmarking Study Using 110 Data Sets. *Entropy*, 26(9), 746
- [25]. Pranjal Atrey, M. P. B., Wu, M., Dutta, S. (2025). Demystifying the Accuracy-Interpretability Trade-Off: A Case Study of Inferring Ratings from Reviews. *DAI Workshop, AAAI-2025*
- [26]. Finn Jacobsen, P. M. J. (2013). *Fundamentals of General Linear Acoustics*. John Wiley & Sons Ltd, United Kingdom.
- [27]. Gafoer, S., & Purbo-Hadiwidjajo, M. M. (1986). The geology of Southern Sumatra and its bearing on the occurrence of mineral deposits. *Bulletin Geological Research and Development Centre*, (12), 15-30.
- [28]. M. C. Daly, B. G. D. H., D. G. Smith. Tertiary Plate Tectonics and Basin Evolution in Indonesia. *Proceedings of Indonesian Petroleum Association, 16th Annual Convention, Indonesia*, 399-428.
- [29]. A. Pulunggono, A. H. S., Christine G. Kosuma. Pre-Tertiary and Tertiary Fault Systems as a Framework of the South Sumatra Basin; A Study of SAR-Maps. *Proceedings Indonesian Petroleum Association, 21st Annual Convention, Jakarta*, 339-360
- [30]. P. Adiwidjaja, G. L. D. Pre-Tertiary Paleotopography and Related Sedimentation in South Sumatra. *Proceedings of Indonesian Petroleum Association, 2nd Annual Convention, of Conference*, 89-103
- [31]. Sosrowidjojo, I. B., & Saghafi, A. (2009). Development of the first coal seam gas exploration program in Indonesia: Reservoir properties of the Muaraenim Formation, south Sumatra. *International Journal of Coal Geology*, 79(4), 145-156
- [32]. Darman, H., & Sidi, F. H. (2000). An outline of the geology of Indonesia. *Indonesian Association of Geologists, Jakarta Selatan*, 11
- [33]. Gafoer, S., Cobrie, T., & Purnomo, J. (1996). The Geology of The Lahat Quadrangle, Sumatera. *Report Geological Research and Development Centre, Bandung*
- [34]. Bishop, M. G. (2000). South Sumatra Basin Province, Indonesia; the Lahat/Talang Akar-Cenozoic total petroleum system. *Open-File Report 99-50-S*, U. S. Department of the Interior, U. S. Geological Survey
- [35]. Pavol Liptai, M. B., Katarína Lukáčová (2015). Influence of Atmospheric Conditions on Sound Propagation - Mathematical Modeling. *Óbuda University e-Bulletin*, 5(1)
- [36]. D. Keith Wilson, C. L. P., Vladimir E. Ostashev (2015). Sound Propagation in the Atmospheric Boundary Layer. *Acoustics Today*, 11(2)
- [37]. Raina Avtar, K., Wankhede, P., & Singh, P. K. Controlled blasting for safe excavation of a portion of irrigation canal in close vicinity of a village, *Proceedings of the conference on Recent Advances in Rock Engineering (RARE 2016)*, 2016/11, 82-84
- [38]. Fernández, P. R., Rodríguez, R., & Bascompta, M. (2022). Holistic Approach to Define the Blast Design in Quarrying. *Minerals*, 12(2), 191
- [39]. Azizi, A., & Moomivand, H. (2021). A New Approach to Represent Impact of Discontinuity Spacing and Rock Mass Description on the Median Fragment Size of Blasted Rocks Using Image Analysis of Rock Mass. *Rock Mechanics and Rock Engineering*, 54(4), 2013-2038
- [40]. Shahrin, M. I., Abdullah, R. A., Jeon, S., Sa'ari, R., Rahim, A., Ghani, J. A. A., & Siti N. Jusoh (2022). Effect of Bench Height to Burden Ratio on Rock Fragmentation Induced by Blasting. *ISRM Regional Symposium - 12th Asian Rock Mechanics Symposium*
- [41]. Moomivand, H., Soltanlinejad, S., & Karwansara, A. M. (2025). Assessment of the optimized stemming length considering rock fragmentation and escape of explosive gases using actual large-scale results. *Results in Engineering*, 25, 103575
- [42]. Uysal, Ö., Arpaz, E., & Berber, M. (2007). Studies on the effect of burden width on blast-induced vibration in open-pit mines. *Environ. Geol.*, 53(3), 643-650
- [43]. Filice, A., Mynarz, M., & Zinno, R. (2022). Experimental and Empirical Study for Prediction of Blast Loads. *Applied Sciences*, 12(5), 2691
- [44]. Faramarzi, ., Ebrahimi Farsangi, M. A., & Mansouri, H. (2014). Simultaneous investigation of blast induced ground vibration and airblast effects on safety level of structures and human in surface blasting. *International Journal of Mining Science and Technology*, 24(5), 663-669
- [45]. Richards, A. B. (2008). Prediction and Control of Air overpressure from Blasting in Hongkong. *Hongkong*

*Geotechnical Engineering Office, Civil Engineering and Development Department, 33*

[46]. Kuzu, C. (2008). The importance of site-specific characters in prediction models for blast-induced ground vibrations. *Soil Dynamics and Earthquake Engineering, 28(5)*, 405-414

[47]. Richards, A. B. (2008). Prediction and Control of Air Overpressure from Blasting in Hong Kong. *Hongkong Geotechnical Engineering Office, 46*.

[48]. Foster, R., & Teague, P. (2004). Prediction Results and Validation of Long Range Noise Propagation from Blast Events. *The Annual Conference of the Australian Acoustical Society, Gold Coast, Australia, 51-56*

[49]. Kazemi, M. M. K., Nabavi, Z., & Khandelwal, M. (2023). Prediction of blast-induced air overpressure using a hybrid machine learning model and gene expression programming (GEP): A case study from an iron ore mine. *AIMS Geosciences, 9(2)*

[50]. Guo, G., Cui, X., & Du, B. (2021). Random-Forest Machine Learning Approach for High-Speed Railway Track Slab Deformation Identification Using Track-Side Vibration Monitoring. *Applied Sciences, 11(11)*, 4756

[51]. Yao, J., & Fang, L. (2021). Building Vibration Prediction Induced by Moving Train with Random

Forest. *Journal of Advanced Transportation, 2021(1)*, 6642071

[52]. Cao, Y., Li, B., Xiang, Q., & Zhang, Y. (2023). Experimental Analysis and Machine Learning of Ground Vibrations Caused by an Elevated High-Speed Railway Based on Random Forest and Bayesian Optimization. *Sustainability, 15(17)*, 12772

[53]. Yan, Y., Guo, J., Bao, S., & Fei, H. (2024). Prediction of peak particle velocity using hybrid random forest approach. *Scientific Reports, 14(1)*, 30793

[54]. Yu, Z., Shi, X., Zhou, J., Chen, X., & Qiu, X. (2020). Effective Assessment of Blast-Induced Ground Vibration Using an Optimized Random Forest Model Based on a Harris Hawks Optimization Algorithm. *Applied Sciences, 10(4)*, 1403

[55]. Sawmliana, C., Roy, P. P., Singh, R. K., & Singh, T. N. (2007). Blast induced air overpressure and its prediction using artificial neural network. *Mining Technology, 116(2)*, 41-48

[56]. Qiu, L., Zhu, Y., Xu, C., Ren, G., Hu, Y., & Liu, X. (2025). Physics-informed neural network optimized by particle swarm algorithm for accurate prediction of blast-induced peak particle velocity. *Intelligent Geoengineering, 2(3)*, 126-140



دانشگاه صنعتی شاهرود

# نشریه مهندسی معدن و محیط زیست

www.jme.shahroodut.ac.ir نشانی نشریه:



انجمن مهندسی معدن ایران

## ارزیابی نویز ناشی از انفجار در معدن روباز: رویکرد مقایسه‌ای با استفاده از مدل‌های تحلیلی و یادگیری ماشین

زینال زینال، نور فوزی ایسنیانو، دلینا موتیارا، دلینا موتیارا، سوفی نوراینی، حسین فاضیله، الفیدا مورالیستا و آندریانتو نوروچمن\*

گروه مهندسی معدن، دانشکده مهندسی، دانشگاه اسلام باندونگ، باندونگ، اندونزی

| اطلاعات مقاله                                                                                            | چکیده                                                                                                                                                                                                                                                                                                                                                                                                                                                                                                                                                                                                                                                                                                                                                                                                                                                                                                                                                                                                                                                                                                                                                                                                                                                                                                                                                                                                                                                         |
|----------------------------------------------------------------------------------------------------------|---------------------------------------------------------------------------------------------------------------------------------------------------------------------------------------------------------------------------------------------------------------------------------------------------------------------------------------------------------------------------------------------------------------------------------------------------------------------------------------------------------------------------------------------------------------------------------------------------------------------------------------------------------------------------------------------------------------------------------------------------------------------------------------------------------------------------------------------------------------------------------------------------------------------------------------------------------------------------------------------------------------------------------------------------------------------------------------------------------------------------------------------------------------------------------------------------------------------------------------------------------------------------------------------------------------------------------------------------------------------------------------------------------------------------------------------------------------|
| تاریخ ارسال: ۲۰۲۵/۰۸/۱۵                                                                                  | <p>انفجار یک عملیات اساسی معدنکاری روباز است که برای شکستن سنگ ضروری است، اما آلودگی صوتی قابل توجهی نیز ایجاد می‌کند. صدای بیش از حد ناشی از انفجار نه تنها سلامت را به خطر می‌اندازد، بلکه مشکلاتی را برای رعایت مقررات ایجاد می‌کند، به ویژه در مناطقی که استانداردهای آکوستیک متفاوت هستند، مانند استفاده اندونزی از استانداردهای dBL و dBA. این تحقیق به نیاز به مدل‌های پیش‌بینی قابل اعتماد و وابسته به زمینه برای صدای انفجار می‌پردازد و هدف آن مقایسه فرمول‌های تحلیلی و تجربی با تکنیک‌های یادگیری ماشین در پیش‌بینی dBA است. اندازه‌گیری‌ها در ۳۰ انفجار در یک معدن زغال سنگ روباز در اندونزی، سوماترای جنوبی، با استفاده از حسگرهای صوتی همگن انجام شد. نقاط داده اندازه‌گیری شده برای فرکانس، dBL و dBA با استفاده از معادلات با داده‌های محاسبه شده مطابقت داده شدند. مدل‌های پیش‌بینی جنگل تصادفی (RF) و شبکه عصبی مصنوعی (ANN) با استفاده از فرکانس اندازه‌گیری شده و dBL به عنوان متغیرهای پیش‌بینی نیز استخراج شدند. نتایج نشان می‌دهد که معادله مشتق شده از فین استفاده شده دقت پیش‌بینی ضعیفی دارد و خطاهای آن بیش از ۸۰٪ است. در میان مدل‌های تحلیلی و تجربی، معادله ۳ با میانگین خطای ۹٪ بهترین عملکرد را داشت، در حالی که یک مدل رگرسیون مکانی-ویژه مبتنی بر اندازه‌گیری‌ها، نرخ خطای بهبود یافته ۵٪ داشت. مدل‌های یادگیری ماشین از همه مدل‌ها بهتر عمل کردند، به طوری که مدل RF میانگین خطای ۲٪ را نشان داد و پایداری و ثبات بالاتری را نشان داد. مدل ANN نیز عملکرد خوبی داشت، اما با تغییرات بیشتر و برخی تخمین‌های بیش از حد.</p> |
| تاریخ داوری: ۲۰۲۵/۰۹/۳۰                                                                                  |                                                                                                                                                                                                                                                                                                                                                                                                                                                                                                                                                                                                                                                                                                                                                                                                                                                                                                                                                                                                                                                                                                                                                                                                                                                                                                                                                                                                                                                               |
| تاریخ پذیرش: ۲۰۲۵/۱۲/۱۴                                                                                  |                                                                                                                                                                                                                                                                                                                                                                                                                                                                                                                                                                                                                                                                                                                                                                                                                                                                                                                                                                                                                                                                                                                                                                                                                                                                                                                                                                                                                                                               |
| <p><a href="https://doi.org/10.22044/jme.2025.16675.3271">DOI:10.22044/jme.2025.16675.3271</a></p>       |                                                                                                                                                                                                                                                                                                                                                                                                                                                                                                                                                                                                                                                                                                                                                                                                                                                                                                                                                                                                                                                                                                                                                                                                                                                                                                                                                                                                                                                               |
| <h3>کلمات کلیدی</h3> <p>نویز انفجار<br/>یادگیری ماشین<br/>تأثیر زیست‌محیطی<br/>مدل‌های پیش‌بینی نویز</p> |                                                                                                                                                                                                                                                                                                                                                                                                                                                                                                                                                                                                                                                                                                                                                                                                                                                                                                                                                                                                                                                                                                                                                                                                                                                                                                                                                                                                                                                               |